

F-51

**SEMI-ANNUAL STATUS REPORT ON
NASA GRANT NAG 1-1087,
"IDENTIFICATION OF AERODYNAMIC MODELS
FOR MANEUVERING AIRCRAFT"**

KU-FRL-872-1

By

Suei Chin and C. Edward Lan

(NASA-CR-186030) IDENTIFICATION OF
AERODYNAMIC MODELS FOR MANEUVERING AIRCRAFT
Semiannual Status Report (Kansas Univ.
Center for Research) 51 p CSCL 01A

N90-25943

Unclas
63/02 0294763

**Flight Research Laboratory
The University of Kansas Center for Research, Inc.
Lawrence, Kansas 66045-2969**

August 1990

Contents

	<u>Page</u>
Nomenclature	ii
Chapter 1: Introduction	1
Chapter 2: Mathematical Development	5
2.1 Aerodynamic Modeling	5
2.2 Least Square Method	12
2.3 Gradient Method	14
2.4 Summary of Numerical Procedure	15
2.5 Indicial Formulation	17
Chapter 3: Results and Discussion	20
3.1 Linear Results	20
3.1.1 Two-Dimensional Flow	20
3.1.2 Three-Dimensional Flow	22
3.2 Nonlinear Results	23
References	27
Figures and Tables	30
Appendix: Successive Fourier Analysis	A.1

Nomenclature

A_j	coefficient of cosine Fourier series
B_j	coefficient of sine Fourier series
C_{ave}	the average value of the constant terms in the harmonic oscillation responses
C_j	coefficient of α^j term in static flow
c_l	2-D lift coefficient.
C_L	3-D lift coefficient.
$C_{L\alpha}$	variation of lift coefficient with respect to angle of attack
C_{Lq}	variation of lift coefficient with respect to pitch rate
d	a constant
E_{ij}	constants associated with the virtual mass effect
H_{ij}	constants in amplitude function to be determined
i	imaginary part of a complex number
j	index
k	reduced frequency ($=\omega l/v_\infty$)
M	Mach number
n	index for reduced frequency, also index for the coefficient in Padé approximants
N	the number of frequency
PD_j	Padé approximants
P_{ij}	coefficients for Padé approximants

t	time
t'	nondimensional time ($=tv_{\infty}/\ell$)
UQVLM	unsteady quasi-vortex lattice method program
v_{∞}	free stream velocity
Greek:	
α	angle of attack ($=\alpha_0 \cos kt'$)
α_1	defined as $\alpha_m + \alpha$
α_0	amplitude of angle of attack
α_m	mean angle of attack
$\dot{\alpha}$	time rate of change in angle of attack
ℓ	reference length
τ	dummy time integration variable
ξ	running variable in time
θ	defined as $\theta = kt'$

Chapter 1

Introduction

Due to the requirement of increased performance and maneuverability, the flight envelope of a modern fighter is frequently extended to the high angle-of-attack regime. Vehicles maneuvering in this regime are subjected to nonlinear aerodynamic loads. The nonlinearities are due mainly to three-dimensional separated flow and concentrated vortex flow that occur at large angles of attack. Accurate prediction of these nonlinear airloads is of great importance in the analysis of a vehicle's flight motion and in the design of its flight control system. As Tobak and Schiff mentioned in ref. 1, the main difficulty in determining the relationship between the instantaneous aerodynamic load on a maneuvering vehicle and the motion variables is that this relationship is determined not only by the instantaneous values of motion variables but also by all of the prior states of the motion up to the current state. Due to advanced computer techniques, one straightforward way is to solve the flow-field problem and the dynamic equation together. For example, a CFD method can be used to solve the Navier-Stokes equations governing the separated flow field. Then the calculated forces and moments are used in the dynamic equations governing the vehicle's motion to calculate motion variables. The motion

variables will change the vehicle's attitude, and thus the forces and moments. Results of repeatedly calculating these coupled equations would be the complete time histories of the aerodynamic response and of the vehicle's motion. Although solving these coupled equations is the exact way to account for the time-history effects in predicting the aerodynamic response to arbitrary maneuvers, this is obviously a very costly approach. In particular, at high angles of attack, the aerodynamic loads depend nonlinearly on the motion variables. Under such conditions, even if the vehicles start from closely similar initial conditions, they can experience widely varying motion histories. Thus, a satisfactory evaluation of the performance envelope of the aircraft may require a large number of coupled computations, one for each change in initial conditions. Further, since the motion and the aerodynamic response are linked together in this approach, there can be no reutilization of the previously obtained aerodynamic reactions.

To avoid the disadvantage of solving the coupled flow- field equations and aircraft's motion equations, an alternate approach is to use a mathematical modeling to describe the steady and unsteady aerodynamics for the aircraft's equations of motion. Ideally, with a mathematical model, an evaluation of the aerodynamic terms specified by the model would be required only once. The specified model can be reutilized to solve the

aircraft's equations of motion over a range of motion variables and flight conditions.

In the classical linear potential flow theory (refs. 2 and 3), researchers in the field of aeroelasticity used the Fourier transform to relate the aerodynamic response of step change in angle of attack of a wing to that of harmonic oscillatory motions. The transient aerodynamic reaction to a step change is termed the "indicial function" and has been calculated for several classes of isolated wings (refs. 2-5). By a suitable superposition (ref. 6) of these results, the aerodynamic forces and moments induced in any maneuvers can be studied (refs. 2 and 3). Tobak has applied the indicial function concept to analyze the motions of wings and wing-tail combinations (ref. 7). Later, based on a consideration of function, Tobak and his colleagues (refs. 1 and 8) have extended the concept of indicial function into the nonlinear aerodynamic regimes. The simplest nonlinear aerodynamic model proposed in ref.1 has been applied by several authors (refs. 9-13) to perform the analysis. However, that simplest model is accurate only to the first order of frequency. It needs to be improved for a more general response.

Aerodynamic forces and moments acting on a rapidly maneuvering aircraft are, in general, nonlinear functions of motion variables, their time rate of change, and the history of maneuvering. How these unsteady aerodynamic forces and moments may be represented becomes uncertain,

in particular at high angles of attack. If the response is measured by wind-tunnel dynamic testing, questions arise as to how the measured time-history data can be analyzed and expressed in a form suitable for flight dynamic simulation. For a certain type of nonlinearities produced in a test with small-amplitude oscillation, the analysis has been accomplished by separating the time-history data into in-phase and out-phase components (ref. 14). When large-amplitude forced oscillations are employed in the wind-tunnel testing at a large mean angle of attack, the aerodynamic phenomena may involve dynamic stall and/or strong vortex flow, with or without vortex breakdown. In this case, higher harmonic components in the aerodynamic response are expected to exist (ref. 15) and the phenomenon of aerodynamic lag may be important. Therefore, a more general modeling technique is needed.

In this research, a numerical method will be developed to analyze the nonlinear and time-dependent aerodynamic response to establish the generalized indicial function in terms of motion variables and their time rates of change.

Chapter 2

Mathematical Development

2.1 Aerodynamic Modeling

Tobak and Schiff (ref. 1), based on a consideration of functional, developed a fundamental formulation of aerodynamic response. For example, the lift response to pitching oscillation may be given in the form of a generalized indicial response as

$$C_L(t) = C_L(0) + \int_0^t C_{L_\alpha} [t, \tau; \alpha(\xi), \dot{\alpha}(\xi), q(\xi), \dot{q}(\xi)] \frac{d\alpha}{d\tau} d\tau + \frac{\ell}{V_\infty} \int_0^t C_{L_q} [t, \tau; \alpha(\xi), \dot{\alpha}(\xi), q(\xi), \dot{q}(\xi)] \frac{dq}{d\tau} d\tau \quad (1)$$

where $\dot{\alpha}$ and q are the time rate of change in angle of attack and the pitch rate, respectively, and t is the time. V is the free stream velocity and ℓ is a reference length. The variable ξ is a running variable in time over the interval 0 to τ . This means that the indicial response depends not only on the current values of motion variables, but also on the past history of these variables. For practical implementation, eq. (1) requires further simplification. By introducing the assumption of a slowly varying motion,

Tobak and Schiff neglected the dependence of the indicial response on $\dot{\alpha}$ and q . A slightly simplified expression of eq. (1) can be written as

$$C_L(t) = C_L(0) + \int_0^t C_{L_\alpha} [t-\tau; \alpha(\tau) \dot{\alpha}(\tau), q(\tau)] \frac{d\alpha(\tau)}{d\tau} d\tau + \frac{l}{V_\infty} \int_0^t C_{L_q} [t-\tau; \alpha(\tau) \dot{\alpha}(\tau), q(\tau)] \frac{dq(\tau)}{d\tau} d\tau \quad (2)$$

Although the form of eq. (2) represents a great simplification over that of eq. (1), the equation still includes the full linear form as a special case.

The main objective in the present investigation is to find a suitable form for the integrand of eq. (2). Then the time response $C_L(t)$ can be calculated through the integration of eq. (2) by substituting the suitable form of C_{L_α} and C_{L_q} . In wind-tunnel testing, q is the same as $\dot{\alpha}$. Since the method developed in this study will be used to analyze wind tunnel data, $\dot{\alpha}$ will be used instead of q in the following investigation and the investigation will be focused on lift force.

In the linear theory (refs. 2 and 3), the aerodynamic response could be separated into a product of an amplitude function and a phase function in harmonic motion. The amplitude function depends on motion variables and their time rate of change. On the other hand, the phase function is a function of frequency and accounts for any phase lag between the response and the excitation. In a two-dimensional linear theory, the phase function

is given by Theodorsen's circulation function (refs. 2 and 3). After response has been obtained at different frequencies with the same amplitude in harmonic oscillation, the phase function can be determined numerically. After use of reciprocal relations (ref. 16), the indicial function can be defined by numerical means. This approach has been used for numerical determination of indicial lift for plunging airfoil in ref. 5 and for plunging wings in ref. 17.

The method for the linear theory will be generalized as follows. Instead of assuming that the aerodynamic response is a product of an amplitude function and a phase function as it is in the linear theory, it is taken to be a sum of the products of amplitude functions and phase functions in harmonic motion; i.e.,

$$C_L = C_0 + \sum_j (\text{amplitude function})_j * (\text{phase function})_j$$

In the linear theory, j equals 1 in the equation. To determine what is the form of the amplitude functions and the phase functions, the aerodynamic response due to harmonic oscillation is assumed to be of the form

$$C_L = F_0 + F(\alpha, \dot{\alpha})\alpha + G(\alpha, \dot{\alpha})\dot{\alpha} \quad (3)$$

and it is defined that

$$\alpha_1 = \alpha_m + \alpha_0 \cos(kt')$$

$$\alpha = \alpha_0 \cos(kt')$$

$$\dot{\alpha} = (-\alpha_0 k) \sin(kt')$$

where k is the reduced frequency, t' is the nondimensionalized time, α_m is the mean angle of attack and α_0 is the amplitude of angle of attack. To find the constant F_0 and functions F and G as functions of $\alpha(t)$ and $\dot{\alpha}(t)$, a functional analysis is needed. However, the following method, "successive Fourier analysis," represents a practical way to accomplish the task. The first step is to Fourier-analyze the response over one period. For simplicity, a Fourier series with three terms will be used to explain the procedure of the modeling. Then

$$\begin{aligned} C_L = & A_0 + A_1 \cos\theta + A_2 \cos 2\theta + A_3 \cos 3\theta \\ & + B_1 \sin\theta + B_2 \sin 2\theta + B_3 \sin 3\theta \end{aligned} \quad (4)$$

The second step is to split the result into the form of eq. (3) with $F(\alpha, \dot{\alpha})$ and $G(\alpha, \dot{\alpha})$ being Fourier-analyzed again. The result after "successive Fourier Analysis" becomes

$$\begin{aligned}
C_L = A_0 + & \{ CC[0,0] + CC[1,0]\alpha + CC[2,0]\alpha^2 \\
& + DC[0,1]\dot{\alpha} + DC[1,1]\alpha\dot{\alpha} + CC[0,2]\dot{\alpha}^2 \} \alpha \\
& + \{ CS[0,0] + CS[1,0]\alpha + CS[2,0]\alpha^2 \\
& + DS[0,1]\dot{\alpha} + DS[1,1]\alpha\dot{\alpha} + CS[0,2]\dot{\alpha}^2 \} \dot{\alpha}
\end{aligned} \tag{5}$$

The detailed procedure of "successive Fourier analysis" is shown in Appendix 1. By collecting the same order terms of α , $\dot{\alpha}$ and their products together, the result of C_L becomes

$$\begin{aligned}
C_L = A_0 + & \{ CC[0,0]\alpha + CS[0,0]\dot{\alpha} \} \\
& + \{ CC[1,0]\alpha^2 + DC[0,1]\alpha\dot{\alpha} + CS[1,0]\alpha\dot{\alpha} \\
& + DS[0,1]\dot{\alpha}^2 \} \\
& + \{ CC[2,0]\alpha^3 + DC[1,1]\alpha^2\dot{\alpha} \\
& + CC[0,2]\alpha\dot{\alpha}^2 + CS[2,0]\alpha^2\dot{\alpha} \\
& + DS[1,1]\alpha\dot{\alpha}^2 + CS[0,2]\dot{\alpha}^3 \}
\end{aligned} \tag{6}$$

It can be seen that for each different frequency k with the same amplitude, there will be different response C_L and different coefficients CC , DC , CS , and DS . To have practical applications, a general representation of these coefficients as a function of reduced frequency at a constant amplitude is needed. From the classical potential theory, it has been found that Padé approximants provide an accurate approximation of the

theoretical phase function. Therefore, Padé approximants will be used for the present model as phase functions to represent coefficients CC, DC, CS, and DS. Equation (6) is a useful form for determining stability derivatives based on forced oscillation tests. For applications to a maneuvering aircraft, the following representation of aerodynamic response based on the generalized indicial lift concept is more convenient.

It is recalled that in the classical airfoil theory the circulatory lift is written as the product of Theodorsen's circulation function and the quasi-steady lift. In the present nonlinear theory, the same form will also be adopted. For this purpose, eq. (4) (or the experimental oscillatory results) is rewritten in a complex form, as follows:

$$C_L = A_0 + (A_1 - iB_1) e^{ikt'} + (A_2 - iB_2) e^{i2kt'} + (A_3 - iB_3) e^{i3kt'} \quad (7)$$

It should be kept in mind that only the real part of the response has physical meaning. The reason to put in the complex form is to benefit from the great mathematical convenience of the $e^{ikt'}$ notation. If α is rewritten as

$$\alpha = \alpha_0 e^{ikt'}$$

and

$$\dot{\alpha} = (i\alpha_0 k) e^{ikt'}$$

then eqs. (6) and (7) and the classical airfoil theory suggest that the response could be put in the following form involving the products of amplitude functions and phase functions as

$$\begin{aligned}
C_L = & C_0(k) \\
& + E_{11}\dot{\alpha} + E_{21}\ddot{\alpha} + C_1 * (H_{11}\alpha + H_{21}\dot{\alpha}) * (1 - PD_1) \\
& + E_{12}\dot{\alpha} + E_{22}\ddot{\alpha} + C_2 * (H_{12}\alpha^2 + H_{22}\alpha\dot{\alpha} + H_{32}\dot{\alpha}^2) \\
& \quad * (1 - PD_2) \\
& + E_{13}\dot{\alpha} + E_{23}\ddot{\alpha} + C_3 * (H_{13}\alpha^3 + H_{23}\alpha^2\dot{\alpha} + H_{33}\alpha\dot{\alpha}^2 + H_{43}\dot{\alpha}^3) \\
& \quad * (1 - PD_3)
\end{aligned} \tag{8}$$

where PD is a Padé approximant with order 2 and is defined as

$$PD_j = \frac{P_{1j} (ik)^2 + P_{2j} (ik)}{P_{3j} (ik)^2 + (ik) + P_{4j}}$$

$E_{11}\dot{\alpha} + E_{21}\ddot{\alpha}$ is the virtual-mass effect and accounts for the noncirculatory lift (ref. 2). In addition, H_{21}, H_{22}, H_{23} , etc., are related to the pitch-rate effect. It should be noted that those terms inside the parentheses following C_1, C_2, C_3 , such as $(H_{11}\alpha + H_{21}\dot{\alpha})$, represent the quasi-steady response and $(1 - PD_j)$ represents the unsteady aerodynamic lag in response. Therefore, the present assumed form for aerodynamic modeling encompasses the classical linear theory.

C_j are the reference values used to normalize the lift given by $A_j - i B_j$ in the least squared-error method. A good choice for C_j is to use the same coefficient in the α_1^j term as in the steady condition. Therefore, j is the index consistent with the exponent of the exponential term in eq. (7). For example if the j 's term in eq. (8) represents the coefficient of $e^{ikt'}$, then j is 1. If the j 's term in eq. (8) represents the coefficient of $e^{i2kt'}$ then j is 2, etc. The first term, $C_0(k)$, in eq. (8) is a constant term, supposedly a function of frequency. From available experimental data (ref. 19), it is found that an averaged constant can be used to represent $C_0(k)$ term as shown in Figure 1 for a delta wing. The unknown coefficients P_{1j} , P_{2j} , P_{3j} and P_{4j} are calculated from the least squared-error method. E_{11} , E_{21} , H_{11} , H_{12} , etc., will be obtained separately by minimizing the sum of squares of errors. This is equivalent to a two-level optimization method to determine the unknowns in eq.(8). That is, E , H , etc., are assumed first. Then P_{1j} , etc., are determined by minimizing the sum of squared errors. The values of E_{11} , H_{11} , etc., are varied next so that the sum of squared errors is minimized. It was found that this approach is more effective in determining a global minimum solution for the unknowns than a straightforward optimization (one level) method because of nonlinearity in the unknowns in the optimization problem. It should be noted that in the literature the phase function has been typically determined by the response to plunging motions. Therefore, those terms associated with $\dot{\alpha}$ in eq. (8) do

not appear. This would very much simplify the mathematics of determining the Padé approximants. The details of the present method are discussed in the following.

2.2 Least-Square Method

By choosing proper values of E_{11} , H_{11} , H_{12} , etc., in eq. (8), the corresponding $A_j - i B_j$ term in eq. (7) is then divided by the amplitude function. The result will appear as

$$\begin{aligned}
 V_j + iW_j &= 1 - \frac{A_j - iB_j}{(\text{amplitude function})_j} \\
 &= \frac{P_{1j} (ik)^2 + P_{2j} (ik)}{P_{3j} (ik)^2 + (ik) + P_{4j}} \quad (9)
 \end{aligned}$$

If both sides of eq. (9) are multiplied by the denominator of the Padé approximant and separated into real and imaginary parts, then

$$\text{Re} \equiv P_{1j}k^2 - P_{3j}V_jk^2 + P_{4j}V_j - W_jk = 0 \quad (10a)$$

and

$$\text{Im} \equiv P_{2j}k + P_{3j}W_jk^2 - P_{4j}W_j - V_jk = 0 \quad (10b)$$

The sum of squared errors is defined as

$$Err = \sum Re(k_i)^2 + \sum Im(k_i)^2 \quad (11)$$

By equating the first derivatives of squared errors (eq. 11) with respect to variables P_{1j} , P_{2j} , P_{3j} and P_{4j} to zero, the unknown coefficients P_{1j} , P_{2j} , P_{3j} and P_{4j} can be determined by

$$\begin{bmatrix} \sum k_i^4 & 0 & -\sum V_i k_i^4 & \sum V_i k_i^2 \\ 0 & \sum k_i^2 & \sum W_i k_i^3 & -\sum W_i k_i \\ -\sum V_i k_i^4 & \sum W_i k_i^3 & \sum (V_i^2 k_i^4 + W_i^2 k_i^4) & -\sum (V_i^2 k_i^2 + W_i^2 k_i^2) \\ \sum V_i k_i^2 & -\sum W_i k_i & \sum (V_i^2 k_i^2 + W_i^2 k_i^2) & \sum (V_i^2 + W_i^2) \end{bmatrix} \begin{bmatrix} P_{1j} \\ P_{2j} \\ P_{3j} \\ P_{4j} \end{bmatrix} = \begin{bmatrix} \sum W_i k_i^3 \\ \sum V_i k_i^2 \\ 0 \\ 0 \end{bmatrix} \quad (12)$$

where i varies over the range of input frequencies, and the mode subscript j on V and W has been omitted.

2.3 Gradient Method

After the unknown coefficients P_{1j} , P_{2j} , P_{3j} and P_{4j} have been found, a one-dimensional gradient method is used to find E and H values which will make the sum of the squared errors minimum. The E or H value is perturbed first by a small amount ΔE or ΔH to find the gradient of the sum

of squared errors. If the gradient tends to reduce the error, then the E or H value is perturbed further until several iterations has been reached (it is set to be 5 iterations in the current program). After that, the same procedure is applied to other E or H. Then the whole procedure is repeated again until several iterations has been reached (it is set to be 10 in the current program).

Finally, the response of C_L is written as

$$\begin{aligned}
 C_L = C_{ave} & \\
 & + E_{11}\dot{\alpha} + E_{21}\ddot{\alpha} + C_1 * (H_{11}\alpha + H_{21}\dot{\alpha}) * (1 - PD_1) \\
 & + E_{12}\dot{\alpha} + E_{22}\ddot{\alpha} + C_2 * (H_{12}\alpha^2 + H_{22}\alpha\dot{\alpha} + H_{32}\dot{\alpha}^2) * (1 - PD_2) \\
 & + E_{13}\dot{\alpha} + E_{23}\ddot{\alpha} \\
 & + C_3 * (H_{13}\alpha^3 + H_{23}\alpha^2\dot{\alpha} + H_{33}\alpha\dot{\alpha}^2 + H_{43}\dot{\alpha}^3) * (1 - PD_3) \quad (13)
 \end{aligned}$$

It is easily seen that each term in the above equation is a product of an amplitude function and a phase function. The procedure to put oscillating response data into the form of eq. (13) is summarized in the next section.

2.4 Summary of Numerical Procedure

Step 1. Steady-state response analysis:

Use Fourier analysis to analyze the steady-flow response over one period which is the same period as in the harmonic motion. Since in the steady flow the only variable in response is α , Fourier cosine series are

used. Then use eq. (A.3) to decompose the response into a polynomial of $\cos(kt')$ or α . If the final result for the steady response is written as

$$C_L = I_0 + I_1\alpha + I_2\alpha^2 + I_3\alpha^3 \quad (14)$$

then the coefficients C_0 , and C_j in eq. (14) are the same value as I_0 , and I_j where $j = 1,2,3$.

Step 2. Unsteady-response analysis:

Use Fourier analysis to analyze the harmonic motion response for different frequencies over one period. For each frequency, the response should be in the same form as in eq. (7).

Step 3. Constant-term analysis:

From step 2, if constant terms appear in the Fourier analysis then C_{ave} is calculated from each constant term due to different frequencies as

$$C_{ave} = \frac{\sum_{n=1}^N A_0(k_n)}{N} \quad (15)$$

where N is the number of frequencies used in step 2 and $A_0(k_n)$ are the constant terms due to different frequencies k_n in Fourier analysis.

Step 4. Amplitude-phase identification:

In this step, the coefficients A_j and B_j calculated from step 2 are put into the form of a product of amplitude functions and phase functions as in eq.(14). The procedure is as follows:

4-a Set the initial guess for E or H values.

4-b Use the least-square method to find unknown coefficients P_{1j} , P_{2j} , P_{3j} and P_{4j} .

4-c Use gradient method to find better E or H values.

Repeat steps 4-a to 4-c until the sum of square errors reached minimum or the setting iteration limit has been reached.

Although three-term Fourier series are used in the above, the procedure is applicable to any number of Fourier terms.

2.5 Indicial Formulation

In linear theory, the reciprocal relations (or Fourier summation) has been used to calculate the indicial response. However, in nonlinear theory those relations can not be applied. As Tobak (ref. 7) mentioned in his paper, the aerodynamic response due to a step change should reach steady-state value asymptotically at subsonic speeds. In linear theory, these

asymptotic relations are represented by exponential functions (refs. 2 and 5), and these exponential functions are calculated through the phase function. Therefore, the phase function in the current nonlinear modeling will be converted into exponential function in time domain but keep the amplitude function unchanged. If eq. (13) is rewritten for m-terms Fourier series as

$$\begin{aligned}
C_L &= C_{ave} \\
&+ E_{11}\dot{\alpha} + E_{21}\ddot{\alpha} + C_1 * (H_{11}\alpha + H_{21}\dot{\alpha}) * (1 - PD_1) \\
&+ E_{12}\dot{\alpha} + E_{22}\ddot{\alpha} + C_2 * (H_{12}\alpha^2 + H_{22}\alpha\dot{\alpha} + H_{32}\dot{\alpha}^2) * (1 - PD_2) \\
&+ E_{13}\dot{\alpha} + E_{23}\ddot{\alpha} + C_3 * (H_{13}\alpha^3 + H_{23}\alpha^2\dot{\alpha} + H_{33}\alpha\dot{\alpha}^2 + H_{43}\dot{\alpha}^3) \\
&\quad * (1 - PD_3) \\
&+ \\
&= C_{ave} + \\
&\quad + \sum_{j=1}^m E_{1j}\dot{\alpha} + E_{2j}\ddot{\alpha} \\
&\quad + (amplitude\ function)_j * (phase\ function)_j
\end{aligned} \tag{16}$$

then by Fourier inversion of the Padé approximants, the integrand in eq. (2) can be obtained from the following expression:

$$\begin{aligned}
C_{L_{indicial}} &= C_1 * (H_{11}\alpha + H_{21}\dot{\alpha}) * (1 - a_{11} e^{-a_{31}t'} - a_{21} e^{-a_{41}t'}) \\
&\quad + C_2 * (H_{12}\alpha^2 + H_{22}\alpha\dot{\alpha} + H_{32}\dot{\alpha}^2) \\
&\quad \quad * (1 - a_{12} e^{-a_{32}t'} - a_{22} e^{-a_{42}t'}) \\
&\quad \quad + \dots \\
&= \sum_{j=1}^m (\text{amplitude function})_j \\
&\quad \quad * (1 - a_{1j} e^{-a_{3j}t'} - a_{2j} e^{-a_{4j}t'}) \tag{17}
\end{aligned}$$

where the coefficients a_{1j} , a_{2j} , a_{3j} and a_{4j} , are calculated from Padé approximants as corresponding indicial response for nonlinear theory is defined as

$$\begin{aligned}
\frac{P_{1j} (ik)^2 + P_{2j} (ik)}{P_{3j} (ik)^2 + ik + P_{4j}} &= \frac{ik a_{1j}}{ik + a_{3j}} + \frac{ik a_{2j}}{ik + a_{4j}} \\
&= \frac{i(jk) a_{1j}}{i(jk) + ja_{3j}} + \frac{i(jk) a_{2j}}{i(jk) + a_{4j}}
\end{aligned}$$

Then the generalized response for arbitrary motion is obtained by time integration of eq. (2).

Chapter 3

Results and Discussion

3.1 Linear Results

Several cases in the two-dimensional and three-dimensional linear flow have been studied to verify the proposed method of aerodynamic modeling.

3.1.1 Two-Dimensional Flow

The first case studied is a 2-D flat plate oscillating in the incompressible flow. The amplitude is 57.3 degree (one radian) in angle of attack for the airfoil. Therefore it oscillates from 57.3 degree of angle of attack to -57.3 degree of angle of attack then back to 57.3 degree of angle of attack for one cycle with respect to midchord. i.e.

$$\alpha_1 = 0.0 + 1.0 \cos(kt') \text{ (in radian)}$$

The steady lift is already known from the linear theory (ref. 2) as $2\pi\alpha$, and the oscillating complex lift is taken from a 2-D unsteady QVLM program (ref. 19) as input data for the current model and for comparison. Through numerical experimentation, it is found that only six frequencies

are needed to have accurate results. Through the modeling procedure as summarized in section 2.4, the lift can be written as

$$c_l = E_{11} \dot{\alpha} + E_{21} \ddot{\alpha} + 2\pi (H_{11}\alpha + H_{21}\dot{\alpha}) (1.0 - PD_1)$$

where

$$PD_1 = \frac{P_{11}(ik)^2 + P_{21}(ik)}{P_{31}(ik)^2 + ik + P_{41}}$$

and the values of coefficients E_{11} , E_{21} , H_{11} , H_{21} and P_{i1} are listed in Table 1. The results for the lift coefficients are plotted in Figure 2 for different numbers of frequencies used. Compared with the aerodynamic responses by the 2-D UQVLM program, the numerical results from modeling show excellent agreement.

Two Mach numbers, 0.2 and 0.4, are chosen in the 2-D compressible flow to verify the current model. A two-dimensional unsteady QVLM (ref. 19) program is again used to calculate the complex lift as input data for the current model and for comparison. The same frequencies as in the incompressible flow are used as input also. The results for coefficients E_{11} , E_{21} , H_{11} , H_{21} and P_{i1} are listed in Table 1. The aerodynamic responses c_l calculated by the model are plotted in Figures 3 and 4 to compare the

results from 2-D unsteady QVLM. These figures show that the numerical results by modeling are very accurate.

3.1.2 Three-Dimensional Flow

The same Mach numbers (includes 0) in the 2-D flow are used in 3-D attached flow to verify the current model. The geometry is a 70 degree delta wing which oscillate from zero degree angle of attack to twenty degree angle of attack i.e.

$$\alpha_1 = 0.1745329 + 0.1745329 \cos kt' \text{ (in radian)}$$

This means that the mean angle of attack is ten degree (0.1745329 radian) and the amplitude of the oscillation is ten degree (0.1745329 radian). The input aerodynamic responses are calculated from a 3-D unsteady QVLM program (ref. 20). In the program, the total lift is the sum of steady lift at the mean angle-of-attack plus unsteady lift. Since the steady lift is the same for every term, only the unsteady lift is used in the modeling and for comparison. Through numerical experimentation, it is found that the responses at low frequencies do not change significantly, which results in inaccurate modeling. To have accurate approximation, high frequencies' responses are needed. Seven reduced frequencies ($k = 0.01, 0.1, 0.2, 0.6, 1.0, 2.0, 2.5$) are used as input data in the 3-D attached flow cases. The

results for the coefficients of the modeling are listed in Table 1. The responses C_L from modeling are plotted in Figures 5 to 7 to compare with the results from 3-D unsteady QVLM program. All of these figures show very good agreement.

3.2 Nonlinear Result

The experimental data (ref. 21) for a 70-degree delta wing in pitching oscillation is used to validate the current aerodynamic model. The angle of attack which describes the pitching motion is given as

$$\alpha_1 = 27.5 - 27.5 \cos kt' \text{ (in degree)}$$

which means the delta wing oscillates from zero degree angle of attack to 55-degree angle of attack then back to zero degree angle of attack for one cycle. The reduced frequency k is nondimensionalized based on wing's root chord. Five sets of data corresponding to five different frequencies are available and they will be used as the input data to calculate the coefficients for the current aerodynamic model. Five terms in the Fourier series are used for the current aerodynamic model. The calculated coefficients for the current aerodynamic model are listed in Table 2, and the response C_L is written as

$$\begin{aligned}
C_L = C_{ave} & \\
& + E_{11}\dot{\alpha} + E_{21}\ddot{\alpha} + C_1 * (H_{11}\alpha + H_{21}\dot{\alpha}) * (1 - PD_1) \\
& + E_{12}\dot{\alpha} + E_{22}\ddot{\alpha} + C_2 * (H_{12}\alpha^2 + H_{22}\alpha\dot{\alpha} + H_{32}\dot{\alpha}^2) * (1 - PD_2) \\
& + E_{13}\dot{\alpha} + E_{23}\ddot{\alpha} + C_3 * (H_{13}\alpha^3 + H_{23}\alpha^2\dot{\alpha} + H_{33}\alpha\dot{\alpha}^2 + H_{43}\dot{\alpha}^3) \\
& \quad * (1 - PD_3) \\
& + E_{14}\dot{\alpha} + E_{24}\ddot{\alpha} + C_4 * (H_{14}\alpha^4 + H_{24}\alpha^3\dot{\alpha} + H_{34}\alpha^2\dot{\alpha}^2 + H_{44}\alpha\dot{\alpha}^3 + H_{54}\dot{\alpha}^4) \\
& \quad * (1 - PD_4) \\
& + E_{15}\dot{\alpha} + E_{25}\ddot{\alpha} \\
& + C_5 * (H_{15}\alpha^5 + H_{25}\alpha^4\dot{\alpha} + H_{35}\alpha^3\dot{\alpha}^2 + H_{45}\alpha^2\dot{\alpha}^3 + H_{55}\alpha\dot{\alpha}^4 + H_{65}\dot{\alpha}^5) \\
& \quad * (1 - PD_5)
\end{aligned}$$

where PDj are the Padé approximants.

The result from modeling is plotted in Figure 8, which shows reasonable agreement with experimental data for each frequency.

3.2.1 Indicial Formulation

Note that eq. (2) is valid for arbitrary motion. To check its validity in the nonlinear theory, two oscillatory cases in the last section will be used. That is, by assuming oscillatory motion in eq. (2), the time-integrated lift response should agree with the forced-oscillation data. As indicated earlier,, the integrand of eq. (2) can be written as follows:

$$\begin{aligned}
C_{L_{indicial}} = & C_1 * (H_{11}\alpha + H_{21}\dot{\alpha}) * (1 - \exp_1) \\
& + C_2 * (H_{12}\alpha^2 + H_{22}\alpha\dot{\alpha} + H_{32}\dot{\alpha}^2) * (1 - \exp_2) \\
& + C_3 * (H_{13}\alpha^3 + H_{23}\alpha^2\dot{\alpha} + H_{33}\alpha\dot{\alpha}^2 + H_{43}\dot{\alpha}^3) * (1 - \exp_3) \\
& + C_4 * (H_{14}\alpha^4 + H_{24}\alpha^3\dot{\alpha} + H_{34}\alpha^2\dot{\alpha}^2 + H_{44}\alpha\dot{\alpha}^3 + H_{54}\dot{\alpha}^4) \\
& \quad * (1 - \exp_4) \\
& + C_5 * (H_{15}\alpha^5 + H_{25}\alpha^4\dot{\alpha} + H_{35}\alpha^3\dot{\alpha}^2 + H_{45}\alpha^2\dot{\alpha}^3 + H_{55}\alpha\dot{\alpha}^4 + H_{65}\dot{\alpha}^5) \\
& \quad * (1 - \exp_5)
\end{aligned}$$

where the functions \exp_j are converted from Padé approximants as

$$\exp_j = a_{1j} e^{a_{3j} * j * t'} + a_{2j} e^{a_{4j} * j * t'}$$

By differentiating with α and $\dot{\alpha}$, C_{L_α} , $C_{L_{\dot{\alpha}}}$ are obtained as follows:

$$\begin{aligned}
C_{L_\alpha} = & C_1 * H_{11} * (1 - \exp_1) \\
& + C_2 * (2H_{12}\alpha + H_{22}\dot{\alpha}) * (1 - \exp_2) \\
& + C_3 * (3H_{13}\alpha^2 + 2H_{23}\alpha\dot{\alpha} + H_{33}\dot{\alpha}^2) \\
& \quad * (1 - \exp_3) \\
& + C_4 * (4H_{14}\alpha^3 + 3H_{24}\alpha^2\dot{\alpha} + 2H_{34}\alpha\dot{\alpha}^2 + H_{44}\dot{\alpha}^3) \\
& \quad * (1 - \exp_4) \\
& + C_5 * (5H_{15}\alpha^4 + 4H_{25}\alpha^3\dot{\alpha} + 3H_{35}\alpha^2\dot{\alpha}^2 + 2H_{45}\alpha\dot{\alpha}^3 + H_{55}\dot{\alpha}^4) \\
& \quad * (1 - \exp_5)
\end{aligned}$$

$$\begin{aligned}
C_{L_s} = & C_1 * H_{21} * (1 - \exp_1) \\
& + C_2 * (H_{22}\alpha + 2H_{32}\dot{\alpha}) * (1 - \exp_2) \\
& + C_3 * (H_{23}\alpha^2 + 2H_{33}\alpha\dot{\alpha} + 3H_{43}\dot{\alpha}^2) * (1 - \exp_3) \\
& + C_4 * (H_{24}\alpha^3 + 2H_{34}\alpha^2\dot{\alpha} + 3H_{44}\alpha\dot{\alpha}^2 + 4H_{54}\dot{\alpha}^3) \\
& \quad * (1 - \exp_4) \\
& + C_5 * (H_{25}\alpha^4 + 2H_{35}\alpha^3\dot{\alpha} + 3H_{45}\alpha^2\dot{\alpha}^2 + 4H_{55}\alpha\dot{\alpha}^3 + 5H_{65}\dot{\alpha}^5) \\
& \quad * (1 - \exp_5)
\end{aligned}$$

The function $C_L(0)$ in eq. (2) includes the initial conditions and virtual mass effect. In the present case, $C_L(0)$ is calculated as

$$\begin{aligned}
C_L(0) = & C_L(t, \alpha(0), \dot{\alpha}(0)) + C_{ave} \\
& + E_{11}\dot{\alpha} + E_{21}\ddot{\alpha} + E_{12}\dot{\alpha}_2 + E_{22}\ddot{\alpha}_2 + E_{13}\dot{\alpha}_3 + E_{23}\ddot{\alpha}_3 \\
& + E_{14}\dot{\alpha}_4 + E_{24}\ddot{\alpha}_4 + E_{15}\dot{\alpha}_5 + E_{25}\ddot{\alpha}_5
\end{aligned}$$

where the subscript to the α -terms indicates the order of the harmonics. For example, α_2 is proportional to the second harmonics. Simpson's 1/3-rule is used to integrate eq. (2). Since the angle of attack is set to be a complex number ($\cos(kt') + i \sin(kt')$) in oscillating cases, only the real part of the integrated lift is taken. The lift by integrating eq. (2) for a 70-deg. oscillating delta wing with frequencies $k=0.098$ and $k=0.165$ are plotted in Figure 9. Compared with the lift from aerodynamic modeling, the integrated lift shows good agreement.

References

1. Tobak, M.; and Schiff, L. B. "Aerodynamic Mathematical Modeling-Basic Concepts." Dynamic Stability Parameters, AGARD-LS-114, 1981.
2. Bisplinghoff, Raymond L.; Ashley, Holt; and Halfman, Robert L. Aeroelasticity. Addison-Wesley Publishing Company, Cambridge, Mass., 1955.
3. Dowell, Earl H. (editor). A Modern Course in Aeroelasticity. Sijthoff & Noordhoff International Publishers, Rockville, Maryland, 1980.
4. Heaslet, M. A.; and Lomax, H. "Two-Dimensional Unsteady Lift Problems in Supersonic Flight." NACA Rep. 945, 1949.
5. Mazelsky, B. "Numerical Determination of Indicial Lift of a Two-Dimensional Sinking Airfoil at Subsonic Mach Numbers from Oscillatory Lift Coefficients with Calculations for Mach Number 0.7." NACA TN 2562, December, 1951.
6. Hildebrand, Francis B. Advanced Calculus for Application. Prentice-Hall, Inc., Englewood Cliff, New Jersey, 1976.
7. Tobak, M. "On the Use of the Indicial Function Concept in the Analysis of Unsteady Motions of Wings and Wing-Tail Combination." NASA Rep. 1188, 1954.

8. Tobak, M.; and Pearson, W. E. "A Study of Nonlinear Logitudinal Dynamic Stability." NASA TR R-209, September, 1964.
9. Katz, J.; and Schiff, L. B. "Modeling Aerodynamic Responses to Aircraft Maneuvers--A Numerical Validation." J.Aircraft, Vol. 23, No. 1, January, 1986, pp. 19-25.
10. Chyu, W. J.; and Schiff, L. B. "Nonlinear Aerodynamic Modeling of Flap Oscillation in Transonic Flow--A Numerical Validation." AIAA Journal, Vol. 21, Jan. 1983, pp. 106-113.
11. Levy, L. L.; and Tobak, M. "Nonlinear Aerodynamics of Bodies of Revolution in Free Flight." AIAA Journal, Vol. 8, Dec. 1970, pp. 2168-2171.
12. Tobak, M.; and Schiff, L. B. "Generalized Formulation of Nonlinear Pitch-Yaw-Roll Coupling, Part 1: Nonlinear Coning-Rate Dependence." AIAA Journal, Vol. 13, March, 1975, pp. 323-326.
13. Tobak, M.; and Schiff, L. B. "Generalized Formulation of Nonlinear Pitch-Yaw-Roll Coupling, Part 2: Nonlinear Coning-Rate Dependence." AIAA Journal, Vol. 13, March, 1975, pp. 327-332.
14. Chambers, J. R.; and Grafton, S. B. "Static and Dynamic Longitudinal Stability Derivatives of a Powered 1/9-Scale Model of a Tilt-Wing V/Stol Transport." NASA TN D-3591, September 1966.

15. Hanff, E. S. "Determination of Non-linear Loads on Oscillating Models in Wind Tunnels." IEEE 10th International Congress on Instrumentation in Aerospace Simulation Facilities, September 1983.
16. Garrick, I. E. "Nonsteady Wing Characteristics." High Speed Aerodynamics and Jet Propulsion, Vol. 7, Princeton, New Jersey, 1957.
17. Chao, C. D.; and Lan, C. E. "Calculation of Wing Response to Gusts and Blast Waves with Vortex Lift Effect." NASA CR-172232, October 1983.
18. Vepa, R. "Finite State Modeling of Aeroelastic Systems." NASA CR 2779, Feb. 1977.
19. Lan, C. E. "The Unsteady Suction Analogy and Applications." AIAA Journal, Vol. 20, No. 12 Dec. 1982, pp. 1647-1656.
20. Lan, C. E. "The Induced Drag of Oscillating Airfoils in Linear Subsonic Compressible Flow." University of Kansas Flight Research Laboratory, Report No. KU-FRL-400, 1975.
21. Soltani, M. R.; Bragg, M. B.; and Brandon, J. M. "Experimental Measurements on an Oscillating 70-Degree Delta Wing in Subsonic Flow." AIAA Paper No. 88-2576, 1988.

Table 1: Results for Linear Flow

2-D Linear Flow										
M	C_1	E_{11}	E_{21}	H_{11}	H_{21}	P_{11}	P_{21}	P_{31}	P_{41}	
0.0	$2\pi/\beta$	0.5	0.0	1.0	0.4449	1.3170	0.2238	2.8422	0.0541	
0.2	$2\pi/\beta$	0.3	0.0	1.0	0.6	0.0775	0.4196	0.1708	0.1322	
0.4	$2\pi/\beta$	0.2651	0.2	1.0	1.4238	1.9738	0.3021	2.7280	0.0483	
3-D Attached Flow										
M	C_1	E_{11}	E_{21}	H_{11}	H_{21}	P_{11}	P_{21}	P_{31}	P_{41}	
0.0	1.6228	0.8	-0.4	1.0	0.7	0.3402	-0.007	5.6880	0.0009	
0.2	1.5358	-1.0	-1.0	1.0	-0.3	-2.559	-0.088	1.3967	0.0009	
0.4	1.4079	-0.8	-1.0	1.0	-0.3	-2.529	-0.208	1.1674	0.0009	

$$\beta^2 = 1 - M^2$$

Table 2: Results for Nonlinear Flow

j	C_j	E_{1j}	E_{2j}	H_{1j}	H_{2j}	H_{3j}	H_{4j}	H_{5j}	H_{6j}
1	1.0162	0.2780	-0.366	-1.046	0.0144	none	none	none	none
2	-5.248	-0.998	-0.997	0.3	-0.499	-0.506	none	none	none
3	-13.68	0.0999	0.4	-0.2	0.0	0.6	0.0	none	none
4	8.7819	-1.070	-1.007	0.2	-0.311	-0.858	0.0148	0.0022	none
5	32.88	-0.097	-0.289	0.0657	-0.203	0.594	.00004	0.0001	0.0
j	P_{1j}	P_{2j}	P_{3j}	P_{4j}	a_{1j}	a_{2j}	a_{3j}	a_{4j}	
1	15.624	1.3858	9.5361	0.0009	1.3964	0.242	-0.001	-0.104	
2	3.5366	0.4202	0.1895	0.0838	0.7546	-19.41	-0.085	-5.193	
3	9.5346	1.1966	9.9619	0.0010	1.2113	-0.254	-0.001	-0.099	
4	-4.315	0.9206	0.1867	0.0288	1.0568	-24.17	-0.029	-5.327	
5	3.2561	1.1818	5.3373	0.033	1.9066	-1.296	-0.042	-0.145	

$C_{ave} = 0.6344$

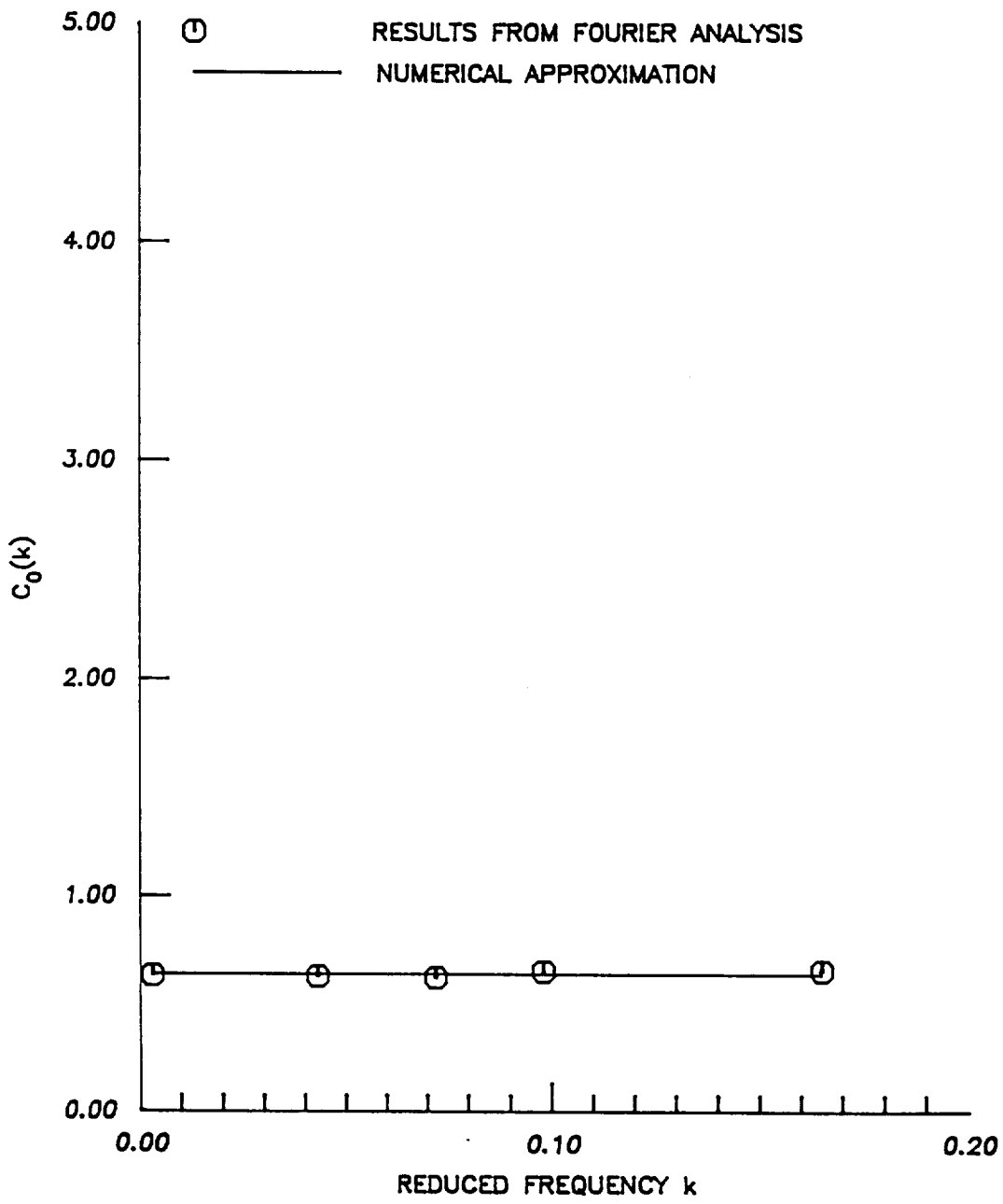
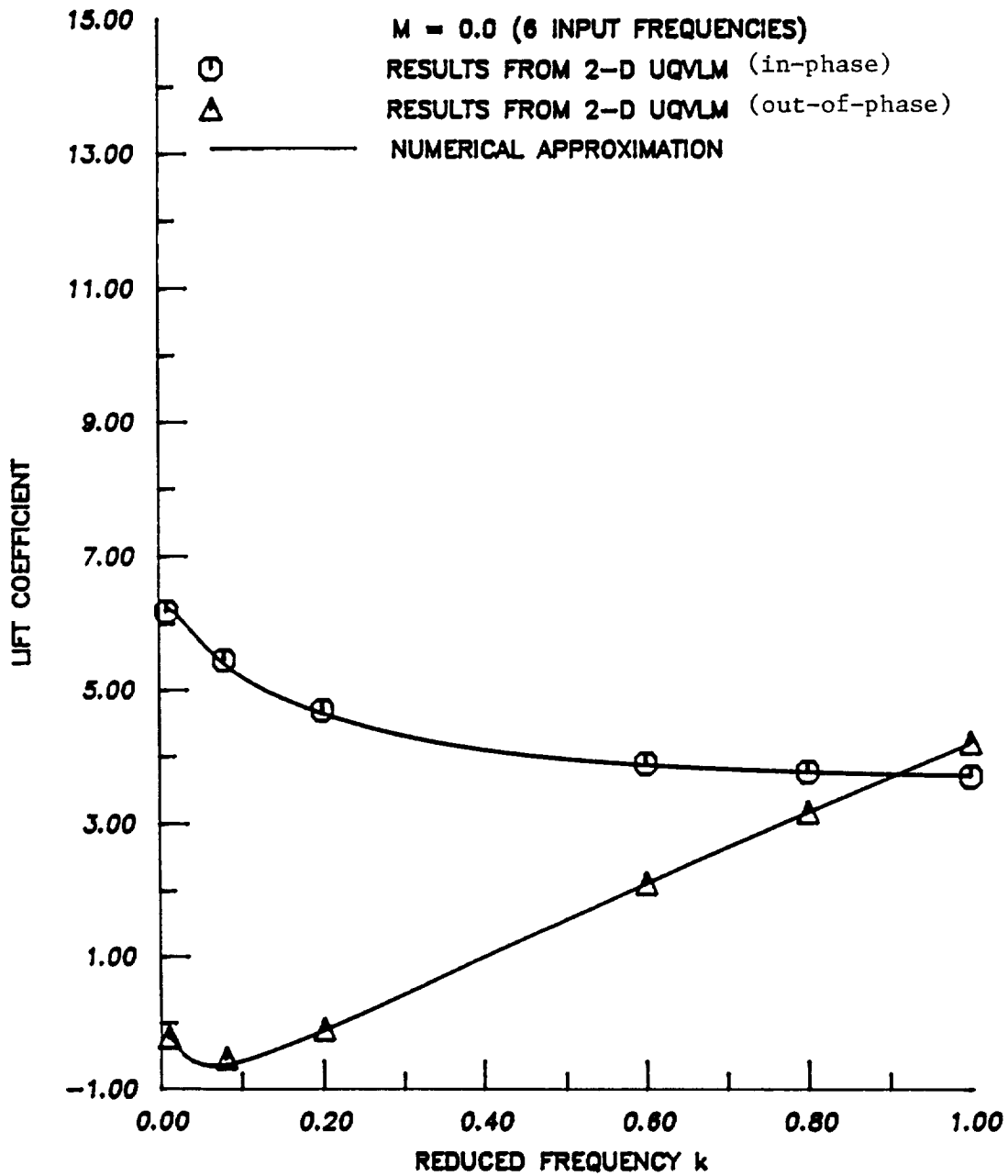


FIG. 1 COMPARISON OF NUMERICALLY APPROXIMATED CONSTANT TERMS WITH RESULTS FROM FOURIER ANALYSIS FOR AN OSCILLATING 70-DEG. DELTA WING



**FIG. 2 COMPARISON OF NUMERICALLY APPROXIMATED COMPLEX
 LIFT COEFFICIENT WITH 2-D UNSTEADY QVLM
 RESULTS AT M=0.0**

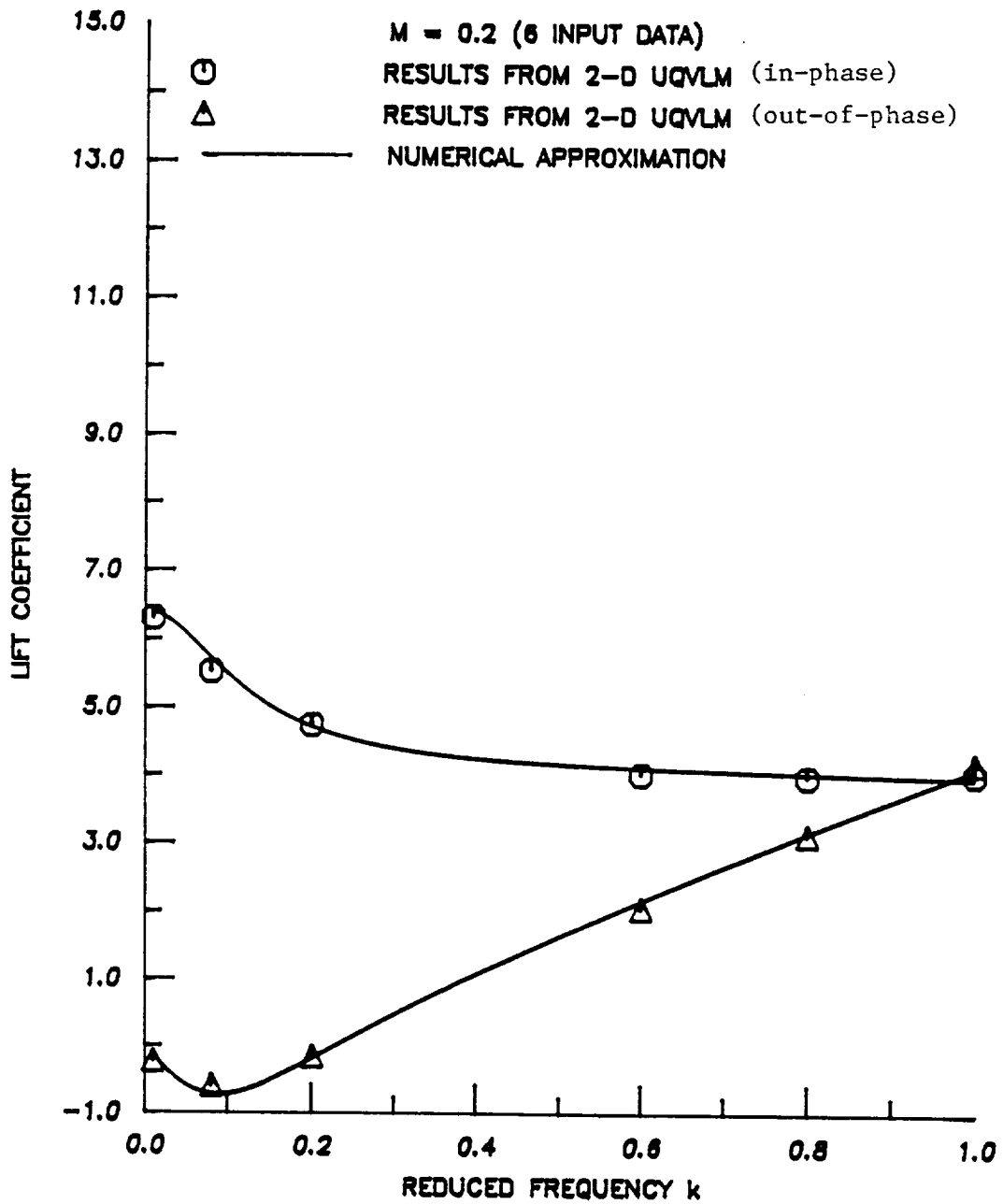
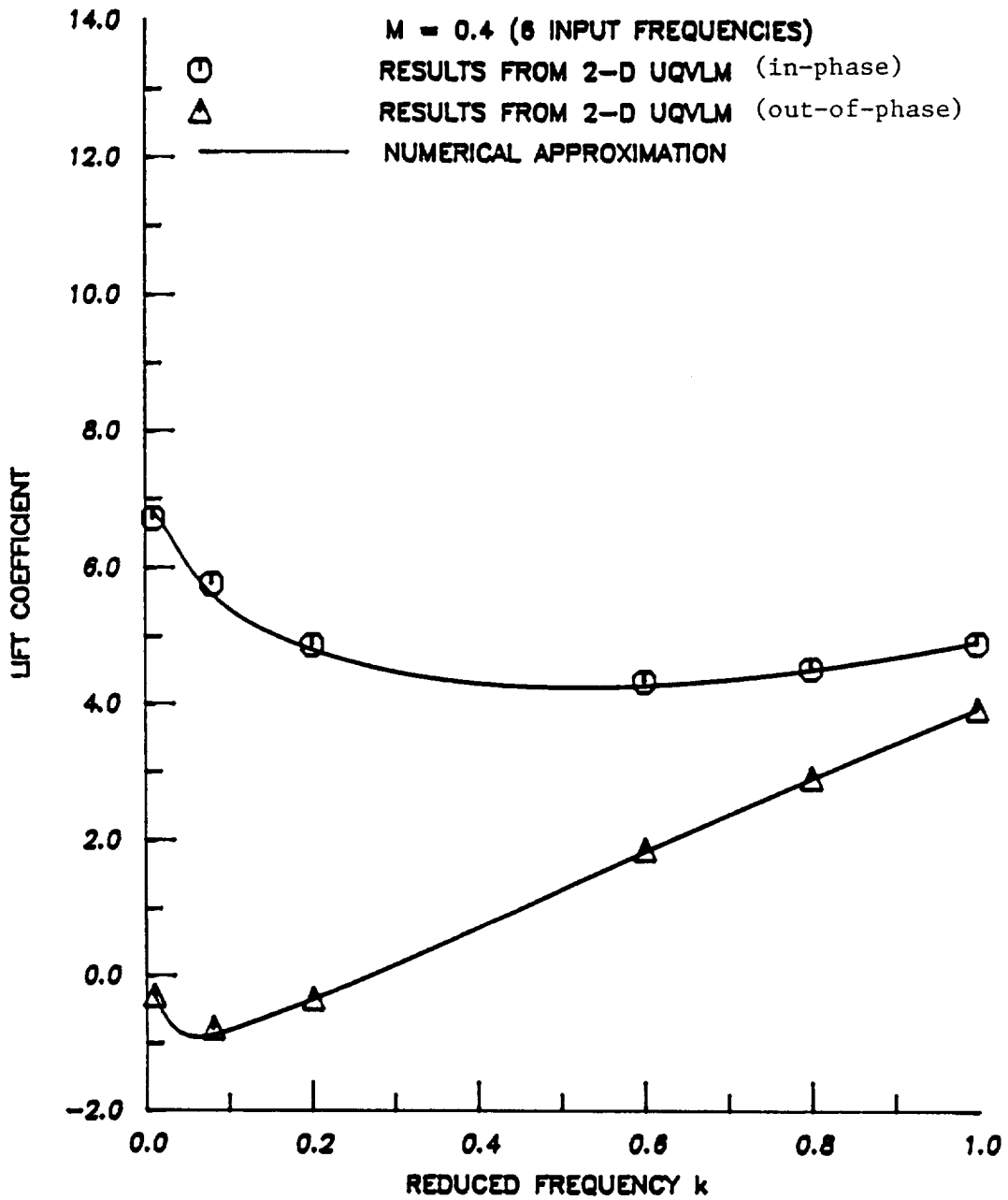


FIG. 3 COMPARISON OF NUMERICALLY APPROXIMATED COMPLEX
LIFT COEFFICIENT WITH 2-D UNSTEADY QVLM
RESULTS AT M=0.2



**FIG. 4 COMPARISON OF NUMERICALLY APPROXIMATED COMPLEX
 LIFT COEFFICIENT WITH 2-D UNSTEADY QVLM
 RESULTS AT M=0.4**

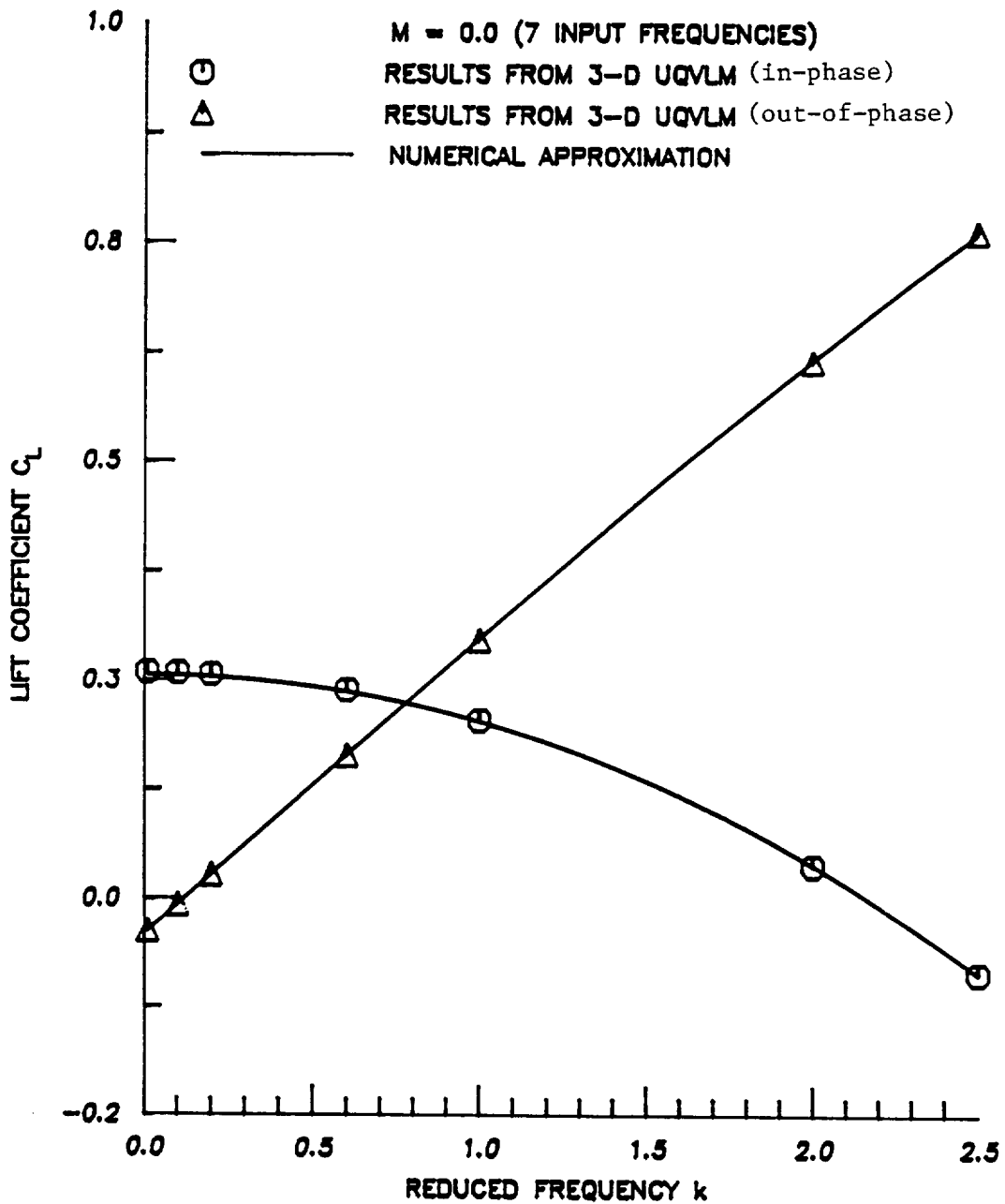


FIG. 5 COMPARISON OF NUMERICALLY APPROXIMATED COMPLEX LIFT COEFFICIENT WITH 3-D UNSTEADY QVLM RESULTS AT M=0.0

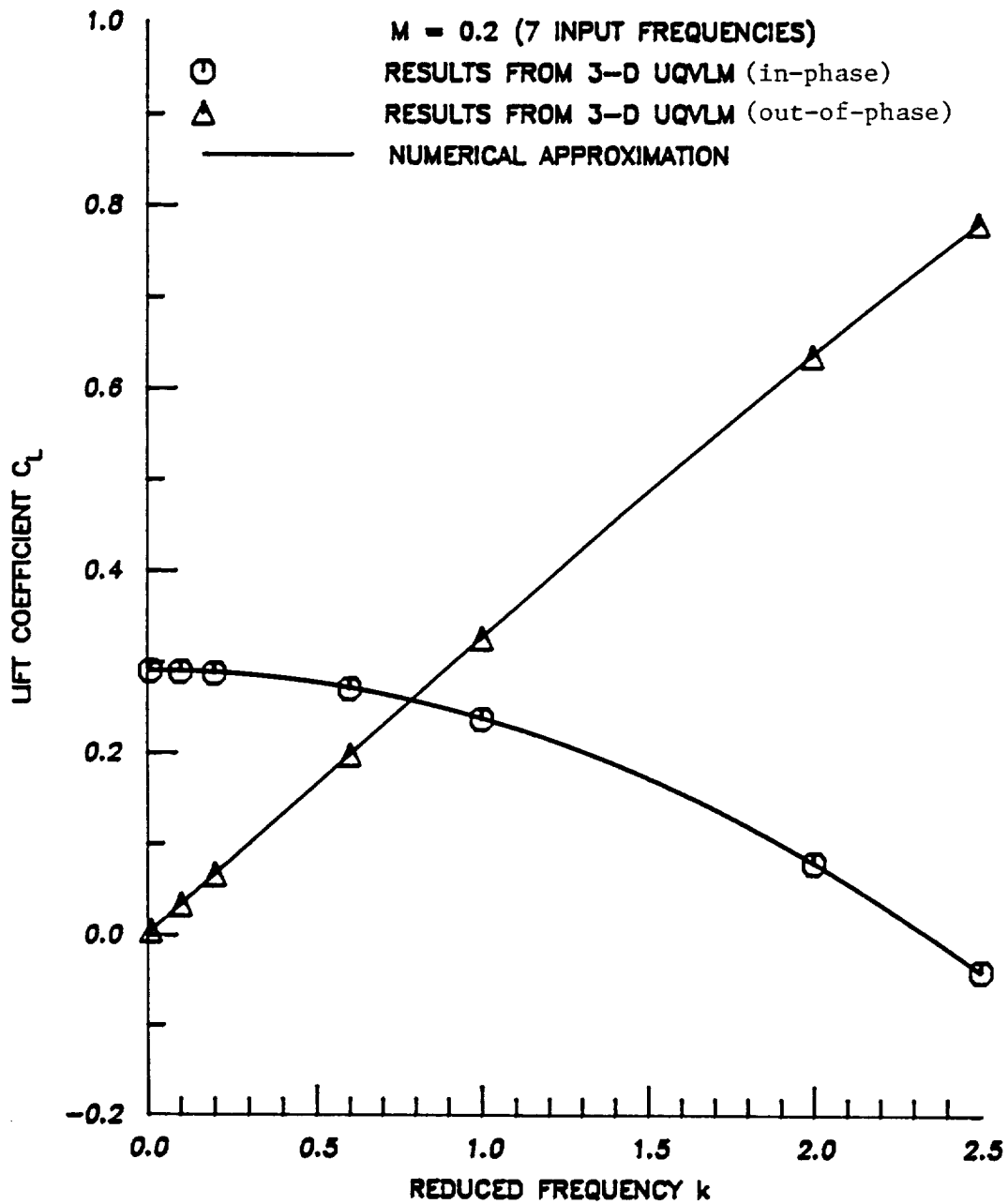


FIG. 8 COMPARISON OF NUMERICALLY APPROXIMATED COMPLEX LIFT COEFFICIENT WITH 3-D UNSTEADY QVLM RESULTS AT M=0.2

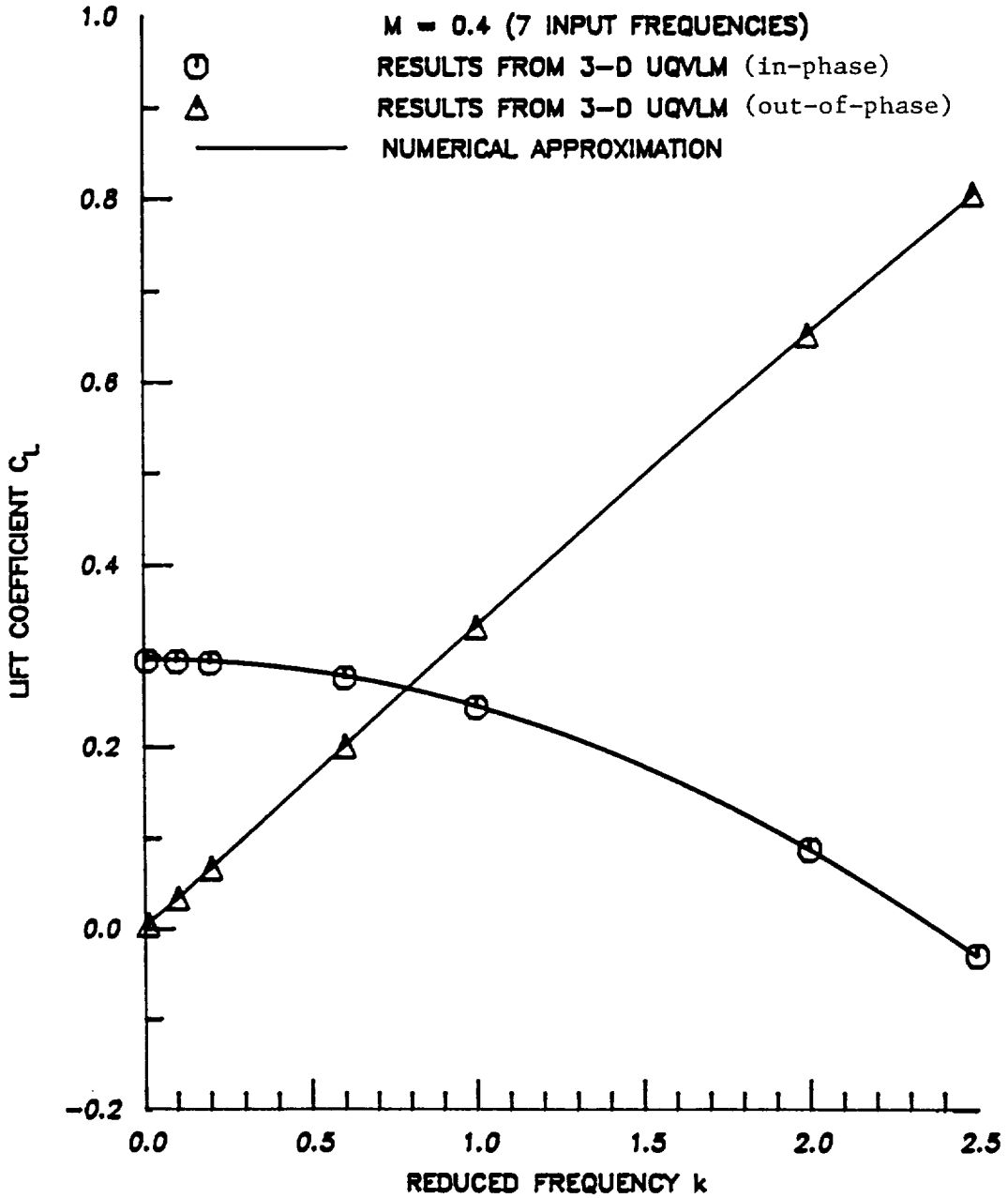


FIG. 7 COMPARISON OF NUMERICALLY APPROXIMATED COMPLEX LIFT COEFFICIENT WITH 3-D UNSTEADY QVLM RESULTS AT $M=0.4$

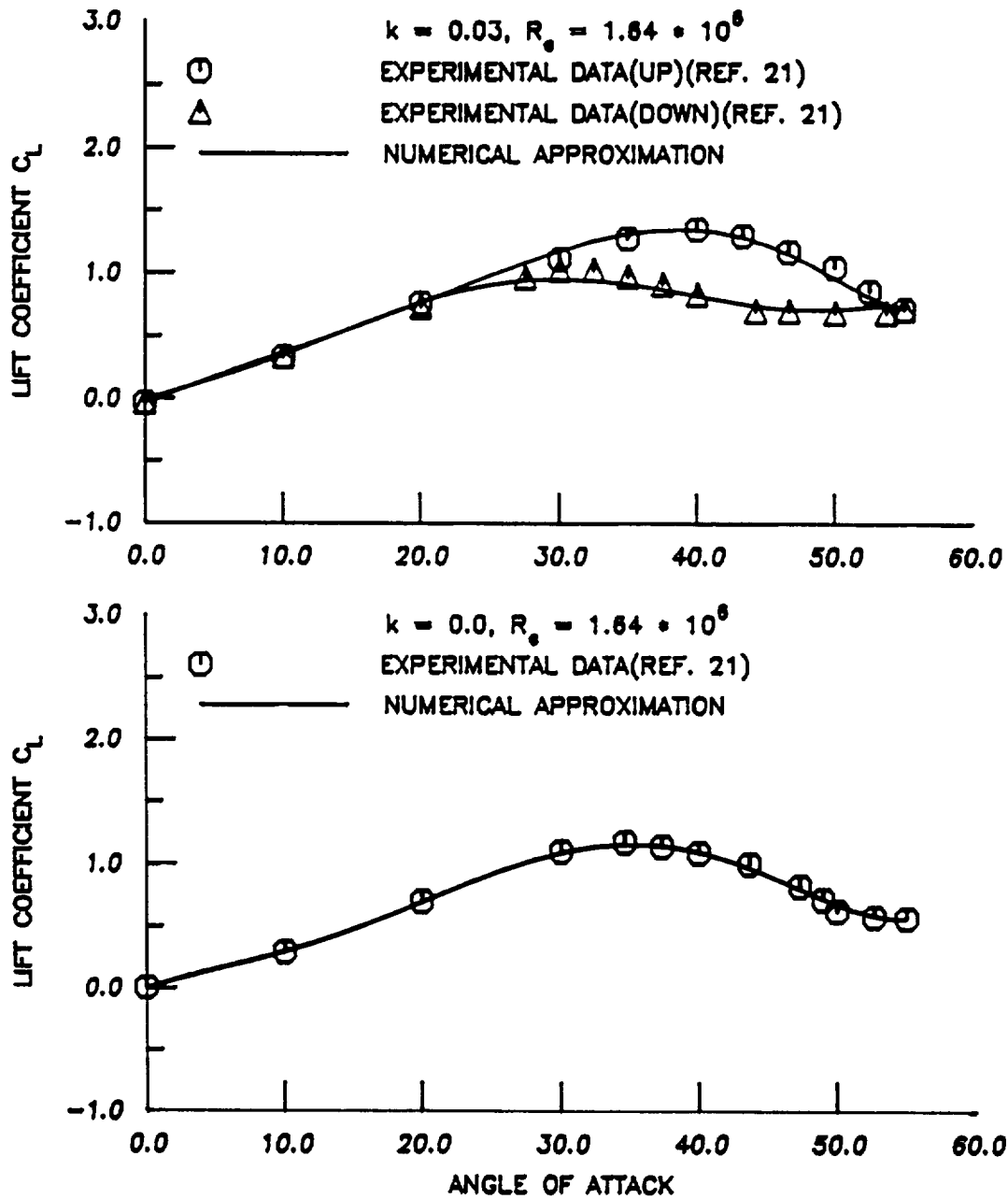
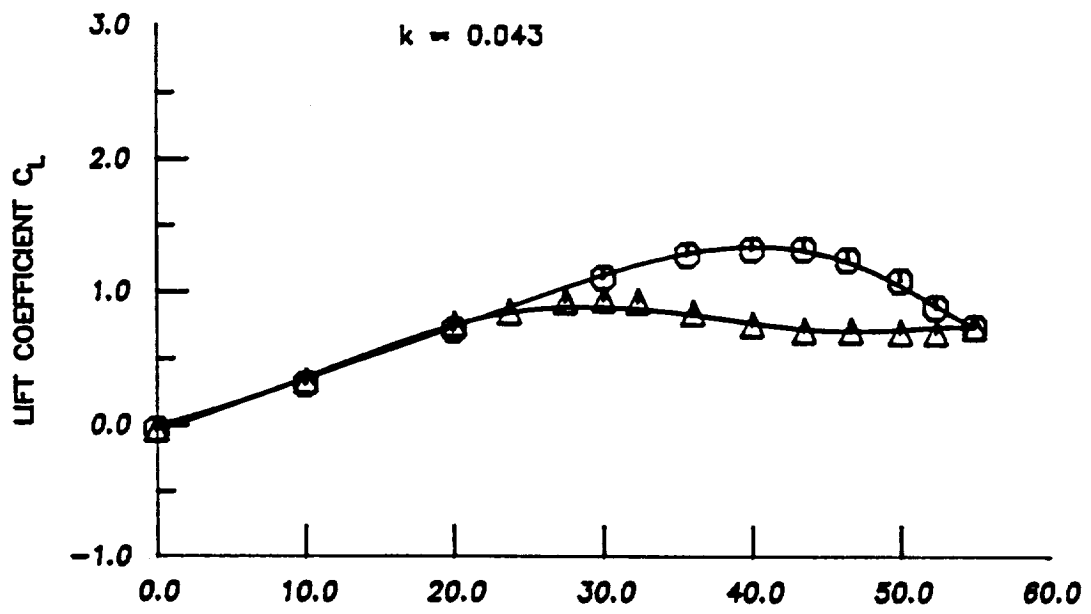
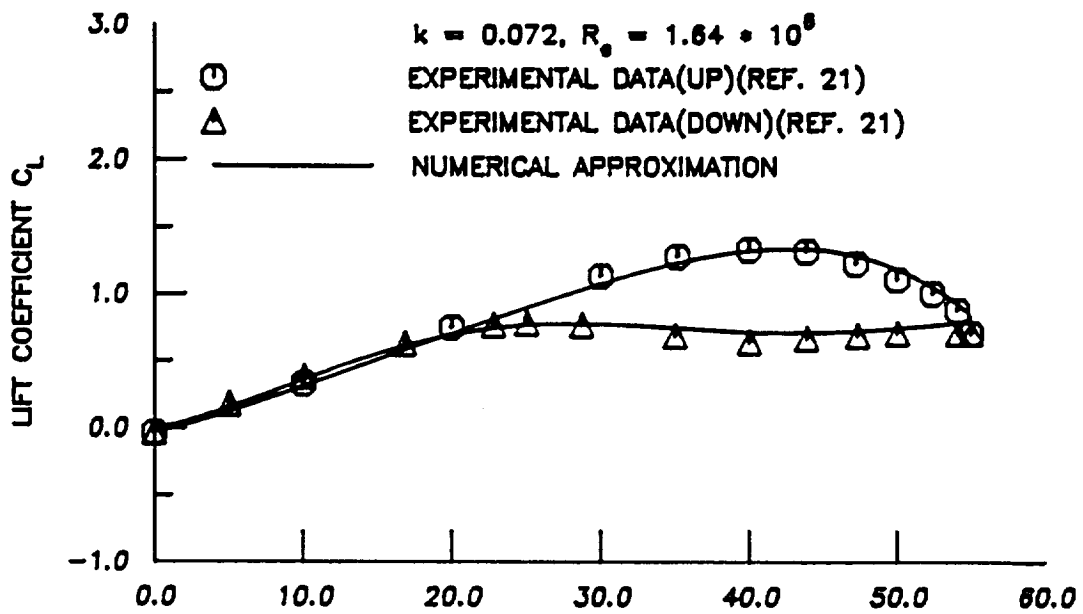
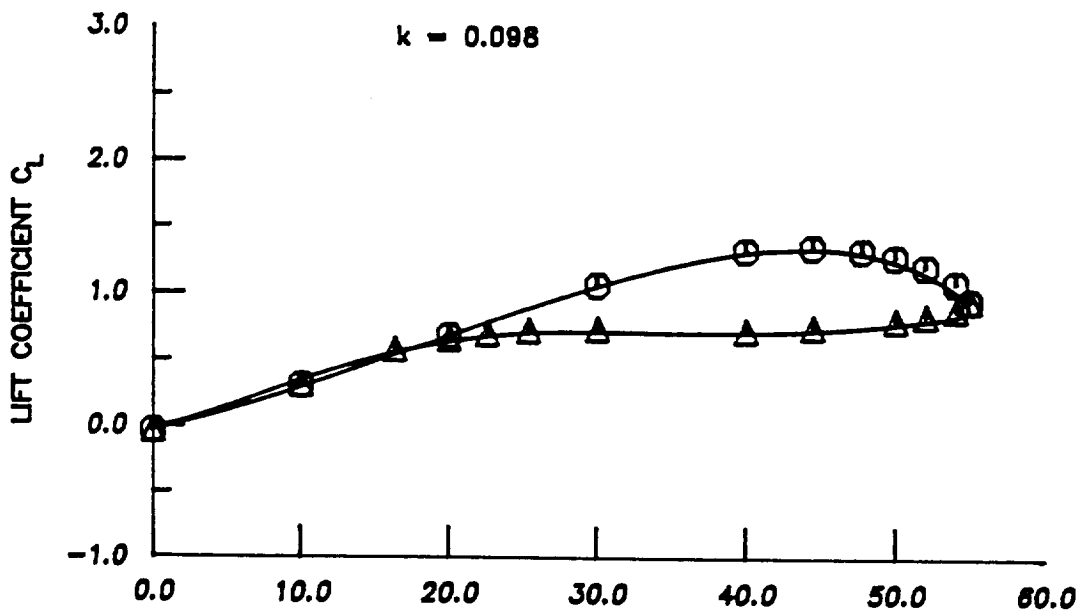
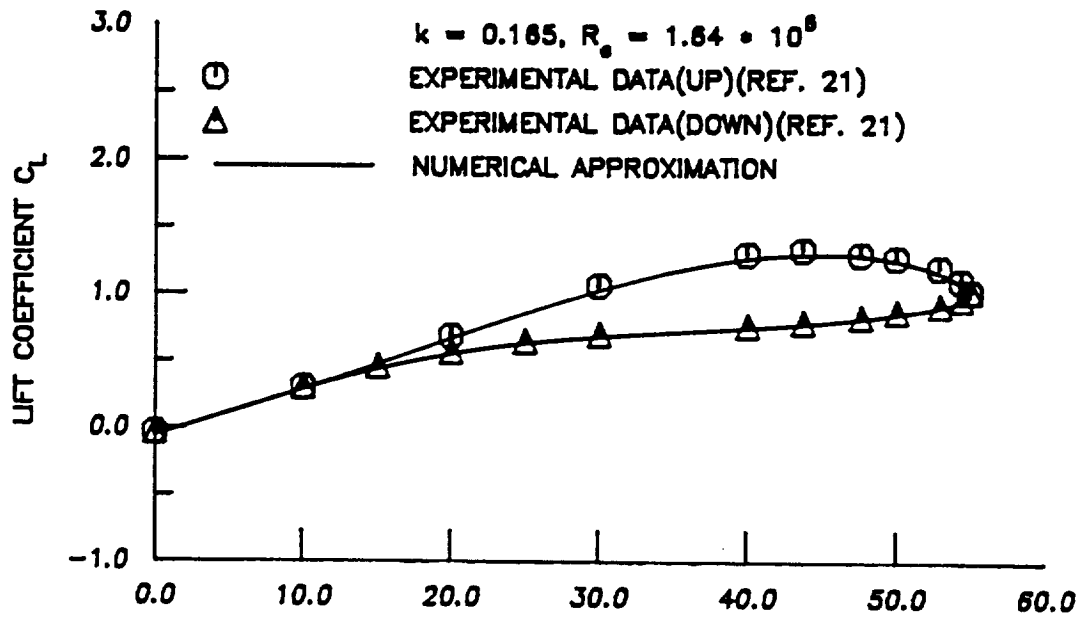


FIG. 8 COMPARISON OF NUMERICALLY APPROXIMATED LIFT COEFFICIENT WITH EXPERIMENTAL DATA FOR AN OSCILLATING 70-DEG. DELTA WING



ANGLE OF ATTACK
 FIG. 8 CONTINUED



ANGLE OF ATTACK
 FIG. 8 CONCLUSION

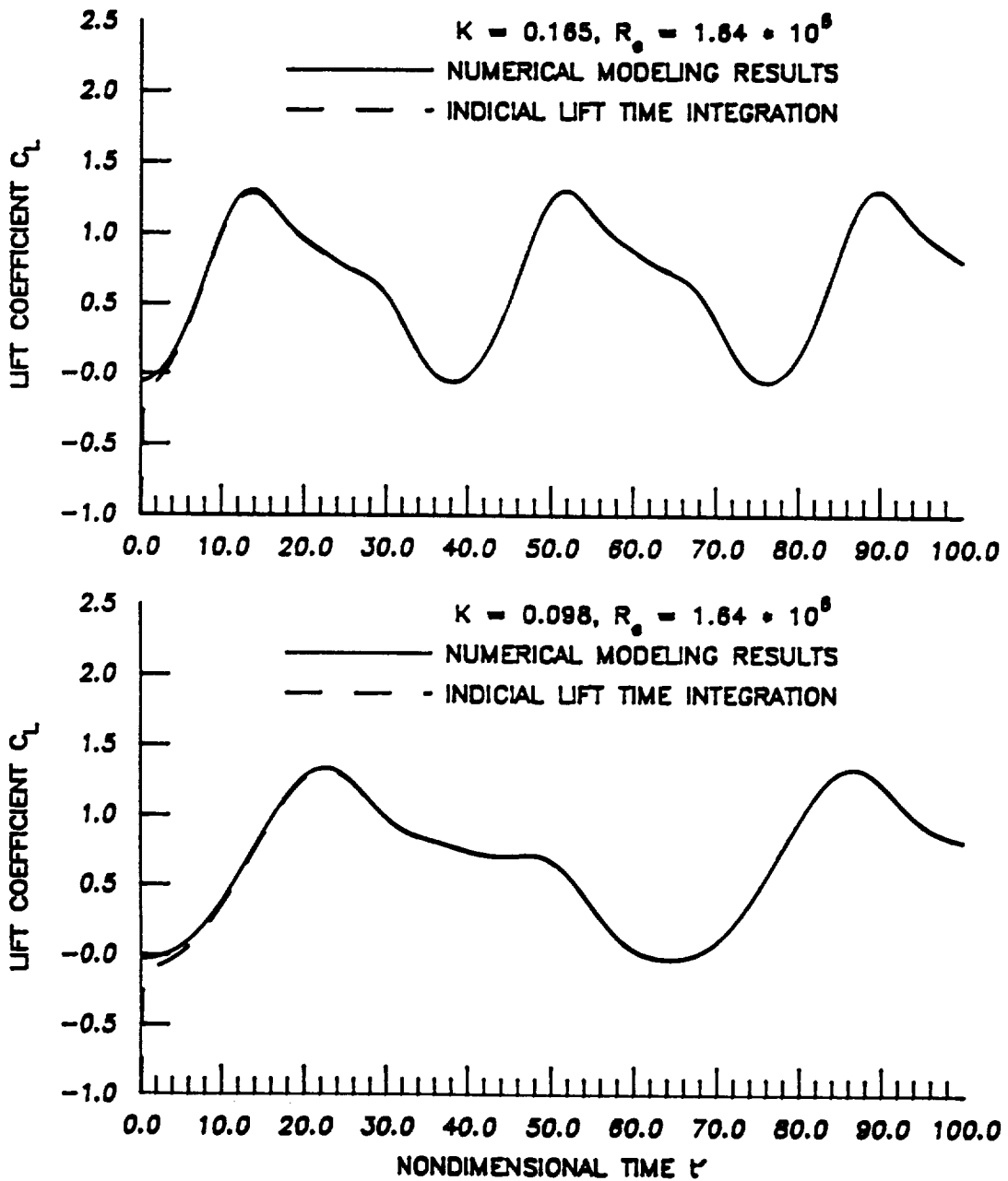


FIG. 9 COMPARISON OF LIFT COEFFICIENT CALCULATED FROM NUMERICAL APPROXIMATED MODELING AND FROM INDICIAL LIFT TIME INTEGRATION FOR AN OSCILLATING 70-DEG DELTA WING

Appendix

Successive Fourier Analysis

The first step of "successive Fourier analysis" is to Fourier-analyze the response over one period. For simplicity, a Fourier series with three terms will be used to explain the procedure of the modeling. Then

$$C_L = A_0 + A_1 \cos\theta + A_2 \cos 2\theta + A_3 \cos 3\theta \\ + B_1 \sin\theta + B_2 \sin 2\theta + B_3 \sin 3\theta \quad (A1)$$

where

$$A_0 = \frac{1}{2\pi} \int_0^{2\pi} C_L \, d\theta \\ A_n = \frac{1}{\pi} \int_0^{2\pi} C_L \cos(n\theta) \, d\theta \\ B_n = \frac{1}{\pi} \int_0^{2\pi} C_L \sin(n\theta) \, d\theta \quad (A2) \\ n=1, 2, 3 \text{ and } \theta=kt'$$

Once the coefficients of A_0 , A_n and B_n have been found, the next step is to split the coefficients into two groups by using the following formulas,

$$\begin{aligned}
\cos n\theta &= C(n,0) \cos^n\theta - C(n,2) \cos^{n-2}\theta \sin^2\theta \\
&\quad + C(n,4) \cos^{n-4}\theta \sin^4\theta + \dots \\
\sin n\theta &= C(n,1) \cos^{n-1}\theta \sin\theta - C(n,3) \cos^{n-3}\theta \sin^3\theta \\
&\quad - C(n,5) \cos^{n-5}\theta \sin^5\theta + \dots
\end{aligned} \tag{A2}$$

where

$$C(n, m) = \frac{n!}{(n-m)! m!} \quad \text{and} \quad n! = 1 * 2 * 3 * 4 * \dots * n$$

Therefore, the response of C_L becomes

$$\begin{aligned}
C_L &= A_0 + A_1 \cos\theta + A_2[\cos^2\theta - \sin^2\theta] \\
&\quad + A_3[\cos^3\theta - 3\cos\theta \sin^2\theta] \\
&\quad + B_1 \sin\theta + B_2[2\cos\theta \sin\theta] \\
&\quad + B_3 [3\cos^2\theta \sin\theta - \sin^3\theta] \\
&= A_0 + [A_1 + A_2 \cos\theta + A_3(\cos^2\theta - 3\sin^2\theta)] \cos\theta \\
&\quad + [B_1 + 2B_2 \cos\theta + B_3 [3\cos^2\theta - \sin^2\theta]] \sin\theta \\
&= A_0 + F(\cos\theta, \sin\theta) \cos\theta + G(\cos\theta, \sin\theta) \sin\theta
\end{aligned}$$

Perform the Fourier analysis again for functions $F(\cos\theta, \sin\theta)$ and $G(\cos\theta, \sin\theta)$ by using Fourier series with the same terms as in the first step. Then

$$F(\cos\theta, \sin\theta) = F_0 + FA_1 \cos\theta + FA_2 \cos 2\theta + FA_3 \cos 3\theta \\ + FB_1 \sin\theta + FB_2 \sin 2\theta + FB_3 \sin 3\theta$$

$$G(\cos\theta, \sin\theta) = G_0 + GA_1 \cos\theta + GA_2 \cos 2\theta + GA_3 \cos 3\theta \\ + GB_1 \sin\theta + GB_2 \sin 2\theta + GB_3 \sin 3\theta$$

where

$$F_0 = \frac{1}{2\pi} \int_0^{2\pi} F d\theta \quad G_0 = \frac{1}{2\pi} \int_0^{2\pi} G d\theta \\ FA_n = \frac{1}{\pi} \int_0^{2\pi} F d\theta \quad GA_n = \frac{1}{\pi} \int_0^{2\pi} G d\theta \\ FB_n = \frac{1}{\pi} \int_0^{2\pi} F d\theta \quad GB_n = \frac{1}{\pi} \int_0^{2\pi} G d\theta \\ n = 1, 2, 3$$

Using eq. (A3) again, then

$$F(\cos\theta, \sin\theta) = F_0 + FA_1 \cos\theta + FA_2 [\cos^2\theta - \sin^2\theta] \\ + FA_3 [\cos^3\theta - 3 \cos\theta \sin^2\theta] \\ + FB_1 \sin\theta + FB_2 [2\cos\theta \sin\theta] \\ + FB_3 [3\cos^2\theta \sin\theta - \sin^3\theta]$$

$$G(\cos\theta, \sin\theta) = G_0 + GA_1 \cos\theta + GA_2 [\cos^2\theta - \sin^2\theta] \\ + GA_3 [\cos^3\theta - 3 \cos\theta \sin^2\theta] \\ + GB_1 \sin\theta + GB_2 [2\cos\theta \sin\theta] \\ + GB_3 [3\cos^2\theta \sin\theta - \sin^3\theta]$$

Therefore

$$\begin{aligned}
C_L = & A_0 + \{F_0 + FA_1 \cos\theta + FA_2 [\cos^2\theta - \sin^2\theta] \\
& + FA_3 [\cos^3\theta - 3 \cos\theta \sin^2\theta] \\
& + FB_1 \sin\theta + FB_2[2\cos\theta \sin\theta] \\
& + FB_3 [3\cos^2\theta \sin\theta - \sin^3\theta]\} \cos\theta \\
& + \{G_0 + GA_1 \cos\theta + GA_2 [\cos^2\theta - \sin^2\theta] \\
& + GA_3 [\cos^3\theta - 3 \cos\theta \sin^2\theta] \\
& + GB_1 \sin\theta + GB_2[2\cos\theta \sin\theta] \\
& + GB_3 [3\cos^2\theta \sin\theta - \sin^3\theta]\} \sin\theta
\end{aligned}$$

All the terms associated with $\cos^n\theta$ on the right hand side of the above equation are divided by $(\alpha_0)^n$ and the terms associated with $\sin^n\theta$ are divided by $(-\kappa\alpha_0)^n$. After rearrangement, the response of C_L becomes

$$\begin{aligned}
C_L = & A_0 + \{CC[0,0] + CC[1,0] \alpha + CC[2,0] \alpha^2 + CC[3,0]\alpha^3 \\
& + DC[0,1] \alpha + DC[1,1] \alpha\alpha + DC[2,1] \alpha^2\alpha \\
& + CC[0,2] \alpha^2 + CC[1,2] \alpha\alpha^2 + DC[0,3] \alpha^3 \} \alpha \\
& + \{CS[0,0] + CS[1,0] \alpha + CS[2,0] \alpha^2 + CS[3,0]\alpha^3 \\
& + DS[0,1] \alpha + DS[1,1] \alpha\alpha + DS[2,1] \alpha^2\alpha \\
& + CS[0,2] \alpha^2 + CS[1,2] \alpha\alpha^2 + DS[0,3] \alpha^3 \} \alpha
\end{aligned} \tag{A4}$$

where

$$\begin{aligned}
 CC[n, m] &= \frac{FA_{n+m}}{[\alpha_0^n (-k\alpha_0^m)]}, & DC[n, m] &= \frac{FB_{n+m}}{[\alpha_0^n (-k\alpha_0^m)]} \\
 CS[n, m] &= \frac{GA_{n+m}}{[\alpha_0^n (-k\alpha_0^m)]}, & DS[n, m] &= \frac{GB_{n+m}}{[\alpha_0^n (-k\alpha_0^m)]}
 \end{aligned}$$

and the coefficients $CC[n,m]$, $DC[n,m]$, $CS[n,m]$ and $DS[n,m]$ are zeros for $n+m \geq 3$. Comparing with eq. (A1), it is obtained that

$$\begin{aligned}
 F_0 &= A_0 \\
 F(\alpha, \dot{\alpha}) &= CC[0,0] + CC[1,0] \alpha + CC[2,0] \alpha^2 \\
 &\quad + DC[0,1] \dot{\alpha} + DC[1,1] \alpha \dot{\alpha} + CC[0,2] \dot{\alpha}^2 \\
 G(\alpha, \dot{\alpha}) &= CS[0,0] + CS[1,0] \alpha + CS[2,0] \alpha^2 \\
 &\quad + DS[0,1] \dot{\alpha} + DS[1,1] \alpha \dot{\alpha} + CS[0,2] \dot{\alpha}^2
 \end{aligned}$$

Finally, collecting the same order terms together, then

$$\begin{aligned}
 C_L &= A_0 \\
 &+ \{ CC[0,0]\alpha + CS[0,0]\dot{\alpha} \} \\
 &+ \{ CC[1,0]\alpha^2 + DC[0,1]\alpha\dot{\alpha} + CS[1,0]\alpha\dot{\alpha} + DS[0,1] \dot{\alpha}^2 \} \\
 &+ \{ CC[2,0]\alpha^3 + DC[1,1]\alpha^2\dot{\alpha} + CC[0,2]\alpha\dot{\alpha}^2 + CS[2,0]\alpha^2\dot{\alpha} \\
 &\quad + DS[1,1]\alpha\dot{\alpha}^2 + CS[0,2]\dot{\alpha}^3 \} \tag{A5}
 \end{aligned}$$